Acousto-Holographic Optical Tweezers

R. Bola,[1,2] D. Treptow,[1,2] A. Marzoa,[1,2] M. Montes-Usategui,[1,2] E. Martin-Badosa[1,2,*]

[1]Optical Trapping Lab – Grup de Biofotònica (BiOPT), Departament de Física Aplicada, Universitat de Barcelona, Martí i Franquès 1, 08028, Barcelona, Spain
[2]Institut de Nanociència i Nanotecnologia (IN2UB), Martí i Franqués 1, 08028, Barcelona, Spain
*Corresponding author: estela.martinb@ub.edu

Received XX Month XXXX; revised XX Month, XXXX; accepted XX Month XXXX; posted XX Month XXXX (Doc. ID XXXXX); published XX Month XXXX

Acousto-optic deflectors allow the creation of multiple optical traps by time-sharing, that is, by rapidly cycling the laser focus between designated spatial locations. The traps thus formed are not permanent. Here, we successfully demonstrate the creation of multiple and permanent traps by means of acousto-optic deflectors driven by specially encoded RF signals. The generation of complex acoustic signals allows us to treat such devices as super-fast spatial light modulators. Using this technique, it is possible to generate several static optical trap arrays and switch them at kilohertz (kHz) rates, allowing independent control of each trap group. Additionally, we discuss the compatibility of this method with precise force and position measurements and the improvement in their frequency bandwidth compared to time-sharing optical tweezers, especially when many objects are trapped.

http://dx.doi.org/10.1364/OL.99.099999

Many experiments require manipulation of objects with multiple optical traps, together with the measurement of their positions or the forces exerted on them. For example, this is the case when we wish to: measure forces at different adhesion sites [1], study multi-particle interactions in colloidal science [2], hold pairs of DNA strands [3], measure forces exerted by the growth cones of differentiating neurons [4], or more generally, grasp large samples or those with complex geometries, such as red blood cells [5], from several sides in order to measure their mechanical properties [6].

The use of spatial light modulators (SLMs) to shape the incoming beam for the dynamic generation of arbitrary light patterns, is a common way to obtain multiple optical traps in so-called holographic optical tweezers (HOTs) [7]. However, the incompatibility of HOTs with laser-based force detection methods that offer high spatial and temporal resolution [8], such as back-focal-plane interferometry (BFPI) [9], has so far limited their applications in precise quantitative experiments. In HOTs, the individual traps become indistinguishable, since the light scattered by all the particles merges into a single intensity pattern at the back focal plane (BFP) of the collection lens. Although there are ways to discriminate the contribution from several traps compatible with high-bandwidth measurements, by polarization [10] or by spatial filtering [11], these are restricted to particular experimental configurations.

As an alternative, video tracking [12], has been used to monitor the displacement of the sample, at the cost of reduced temporal resolution. High-speed cameras can reach frame rates of a few kilohertz, compared to the hundreds of kilohertz of quadrant photodiodes. Additionally, camera-based detection systems are dependent on an off-line calibration and they need to process large data streams. However, they allow the parallelization of experiments, being able to simultaneously measure at many positions.

Another approach is to share a single laser between optical traps by quickly changing the angular deflection of the beam by means of acousto-optic deflectors (AODs) [13]. In this way, the information of each trapped object becomes temporally distinguishable at the BFP when there is proper synchronization [14]. This compatibility with laser detection methods has made this the preferred technique for accurate position and stiffness calibration at multiple sites in the sample plane. Compared to SLMs, AODs are extremely fast devices (modulation rates in the hundreds of kHz range) which allow feedback control and real time manipulation. However, traps are not permanent and while the laser is off, the particle diffuses away from the trap location. This ultimately limits the accuracy to which the particle can be positioned, or its position measured.

Fluctuations in position or trap stiffness can be significant, especially in single-molecule experiments [15]. Even though hundreds of time-multiplexed optical traps have been generated with rapid AODs [16], there is considerable limitation on the number of traps when measuring with laser-based detection methods and accuracy is a concern [17]. Additionally, since the laser is visiting one trap each time, the effective sampling frequency of each of the N trapped objects is reduced by a factor of N, which leads to aliasing effects in the power spectrum and a loss of information at high frequencies [18]. Therefore, the sampling rate of the detector should be increased as the number of time-

shared traps increases. This quickly becomes limited by the finite sensor bandwidth, especially at IR wavelengths.

To overcome this issue, since many experiments do not require simultaneous measurements in all the traps, we propose an alternative method where holographic traps could be created for manipulation, while multiplexing of the laser would allow selective, accurate detection at defined locations.

This idea of time-multiplexing different trap configurations has already been implemented using a combination of two devices, for example, galvanometric mirrors and SLMs. However, it has only been used to increase the field-of-view of a single SLM [19], or with SLMs and AODs [20, 21] to correct for aberration in a multiplexed array of optical traps.

Here, we propose an approach that does not need separate deflection and modulation devices. We show that the same pair of AODs can be used to generate, and multiplex, permanent trap arrays. Commonly, when using AODs, a high-power sinusoidal radio frequency (RF) signal drives a piezoelectric actuator within the AOD device creating a traveling sound wave that modulates the crystal refractive index. Once the laser propagates through this periodic index modulation, an initial diffracted order appears at an angle that is proportional to the frequency of the signal.

Considered carefully, this is not too different from the way certain SLMs modulate the amplitude or phase of the laser wavefront. That is also achieved by inducing changes in the refractive index of the material filling the pixels of the device. If, instead of introducing the pure sinusoidal signal that produces a deflection, we compute and encode the amplitude and phase information of a desired diffractive optical element (DOE) within a more complex RF signal, then the AOD cell would diffract the light just as a physical diffraction pattern would [22-24]. We call this approach acousto-holographic optical tweezers (AHOTs). It allows the generation of permanent holographic traps, but also changes of the desired configuration at super-fast rates: much higher than the typical refreshing times of SLMs (hundreds of Hz at the most). Additionally, it permits the simultaneous modulation of the wavefront amplitude, which current SLMs do not.

Acousto-optic holograms that spatially modulate the amplitude and phase of a passing beam of light can be synthesized by driving the AOD cell with a modulated sinusoidal signal of the form:

$$u(t) = A(t)\, sin(2\pi f_c t + \varphi(t)) \qquad \textbf{(1)}$$

with time-varying amplitude $A(t)$ and phase modulation $\varphi(t)$. The frequency f_c is the central driving frequency of the AOD, around which the diffraction efficiency is optimal. The spatial index perturbation (diffraction grating) along the acoustic path $n(x,t)$ takes a similar form to that of the driving signal, albeit with a material-specific factor, γ [22]:

$$n(x,t) = \gamma A\left(t + \frac{x}{v}\right) sin\left[\varphi_L\left(t + \frac{x}{v}\right) + \varphi\left(t + \frac{x}{v}\right)\right] \qquad \textbf{(2)}$$

where

$$\varphi_L(t + x/v) = 2\pi f_c[t + x/v] \qquad \textbf{(3)}$$

and v is the acoustic speed of the moving grating in the x-direction. A collimated light beam of wavelength λ crossing an AOD of thickness d experiences a spatial phase modulation due to the optical path differences induced by the index variation. When the beam, $G(x,t)$, is incident perpendicular to the direction of the acoustic propagation, x, the modulated beam, $M(x,t)$, can be written as:

$$M(x,t) = G(x,t) exp\left(i\frac{2\pi d n(x,t)}{\lambda}\right) \qquad \textbf{(4)}$$

The AODs used in this work operate within the Bragg regime, which means that most of the energy is concentrated in the first diffraction order. This allows us to simplify Eq. 4 utilizing the Jacobi-Anger identity, by splitting the exponential term into the different diffraction orders [22]. By neglecting all but the first, we obtain:

$$M(x,t) \approx \frac{\gamma d\pi}{\lambda_0} G(x,t) A\left(t + \frac{x}{v}\right) \cdot exp\left\{i\varphi(t + \frac{x}{v})\right\} exp\left\{i\varphi_L(t + \frac{x}{v})\right\} \qquad \textbf{(5)}$$

That is to say, the amplitude and phase modulation of the beam are equal to the amplitude and phase modulation of the electronic driving signal. Therefore, arbitrary amplitude and phase holograms can be displayed on the AOD by controlling the complex modulation of the AOD driving signal as we now explain (Fig. 1). For optical tweezers applications, the intensity distributions are typically sparse, consisting of discrete focused spots arranged in different configurations, such as forming a 2D array.

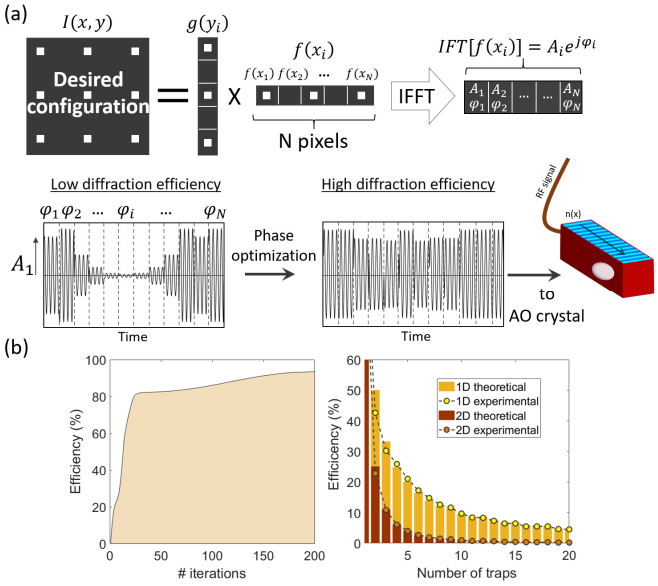

Fig. 1. (a) Flux diagram of the custom algorithm to calculate the complex RF signal. (b) (Left) Evolution of the efficiency optimization process when implementing the Gerchberg-Saxton algorithm. (Right) efficiency as a function of the number of traps when efficiency optimization is not applied. All efficiency values are referenced to a pure sinusoid (75%)

The procedure for generating the trap configurations is as follows: first the intensity pattern is decomposed into two 1D digital vectors of N elements whose product reproduces the desired intensity distribution (a requirement we discuss below). Then, since both AOD planes are conjugated to the back aperture of the microscope objective, an Inverse Discrete Fourier Transform is performed to calculate the required hologram. To encode these complex values into the RF signal, the laser beam size is divided

into the same number of segments or pixels, N, which is only limited by the sample rate of the arbitrary waveform generator (AWG) (much larger than the number of traps). The segments consist of a pure sinusoid of the same RF frequency (the AOD central frequency), but whose amplitude and phase are those calculated for the hologram pixels. Note that the AOD cell is capable of both amplitude and phase modulation [25]. However, since the diffraction efficiency of AODs is proportional to the RF signal average power, the Gerchberg-Saxton (GS) iterative algorithm is used to obtain an almost phase-only hologram with very small amplitude variations [26].

Alternatively, the RF signal can be calculated using the fact that AODs satisfy the superposition principle (intermodulation effects are negligible). Considering that each desired focus position corresponds to a fixed frequency, the complex RF signal is simply the sum of sinusoidal functions, each with its own frequency [22-24]. This second way of encoding information does not show sudden phase and amplitude jumps due to pixel discretization (see Fig. 1(a)), which means there are no replicas at the boundaries of the field of view. On the other hand, the degrees of freedom of this method are less than those of the GS algorithm and the obtained experimental efficiency was lower. However, we used a relatively simple algorithm that is open to improvement.

Unfortunately, we have encountered two important difficulties that do not arise with traditional SLMs. A 2D AOD is formed of two separate 1D deflectors placed orthogonally, one after the other. Thus, the driving signals can encode *2N* values instead of *NxN*, and this restriction limits the modulation configurations to those that are mathematically separable in *x* and *y*. Therefore, the intensity distribution at the sample plane, i.e., the desired trap configuration, *I(x,y)*, needs to be expressed in terms of two functions *f(x)* and *g(y)* such that $I(x,y)=f(x)\cdot g(y)$ (first step in Fig. 1). If we require a more general light field, *I(x,y)* should be decomposed as an incoherent superposition of products of separable functions $f_i(x)$ and $g_i(y)$, which would then be displayed and integrated over time at the cost of reconstruction speed.

Any function can be synthesized by means of separable functions through singular value decomposition [27]. However, for simplicity, here we focus only on trap configurations that are separable. In addition, AHOTs do not permit 3D manipulation, as the information is encoded in a traveling sound wave. AODs only produce a stable intensity pattern at a Fourier conjugate, since the motion of the hologram appears as a pure phase term due to the shifting property of Fourier transforms [22].

Different combinations of trap configurations were created in a custom optical tweezer setup, built on an inverted Nikon TE-2000E microscope, as illustrated in Fig. 2. The trapping laser ($\lambda = 1064$ nm, IPG YLM-5-1064-LP) is sent directly through two dichroic mirrors (M1 and M2) to the entrance window of two 1D AODs. Only the first diffracted order of each deflector is selected, in such a way that the beam leaving the y-AOD enters the x-AOD by means of a telecentric relay (lenses L1 and L2, 1x magnification), which conjugates both devices. The diffracted order is then expanded through another 4f system (lenses L3 and L4, 1.6x magnification), in order to fit the entrance pupil of the microscope objective (MO), which additionally properly conjugate the deflection plane of each AOD with the entrance pupil, avoiding beam vignetting. The laser beam then enters the microscope through the epi-fluorescence port and a dichroic mirror (DM) reflects it up towards a water immersion microscope objective (Nikon Plan Apo 60x, NA 1.2), which focuses the laser beam on the sample, creating the desired optical trap patterns in the focal plane. Complex RF signals were synthesized, amplified and sent to the AODs using an AWG (Rigol DG5102) and properly dimensioned RF amplifiers (MiniCircuits).

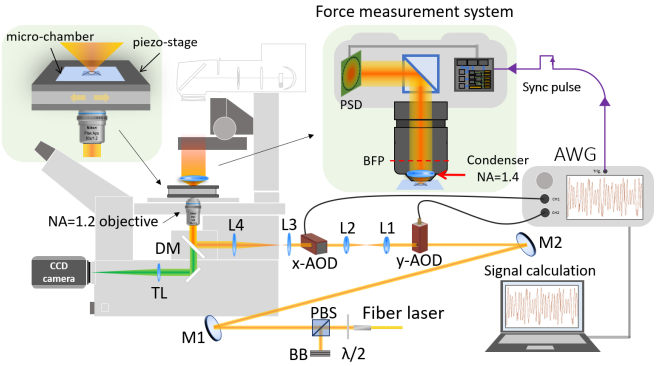

Fig. 2. Experimental setup for the generation of acousto-holographic optical traps, combined with a momentum-change-based direct force measurement system.

In order to dynamically change the intensity patterns, different holograms were stored into the AWG internal memory, and then streamed sequentially at the desired rate, maximum at 100 KHz.

The resulting trap patterns were of high quality. When a phase-only SLM is used, ghost traps may appear due to the restricted modulation capacity. We attribute such high reconstruction quality to the ability of AODs to also modulate the amplitude. Additionally, all traps were simultaneously present, which can be deduced from the existence of interference fringes at the BFP of the condenser lens.

To confirm the capacity of AHOTs to address single object information, we performed a drag force experiment. Two sets of optical traps were generated: one formed by two traps separated 20 μm in the *x*-direction, and the other by four traps placed at the corners of a 20 x 20 μm square (Fig. 3(a)). The experiment consisted of trapping several combinations of 1.17 and 3 μm polystyrene micro-beads, while a measuring a controlled external force generated by the movement of a piezoelectric stage (Piezosystem Jena, TRITOR 102 SG).

The total lateral force exerted by the whole set of holographic traps was determined without a specific calibration, by quantifying changes in the beam's linear momentum. Such changes can be precisely measured at the BFP of the condenser lens by capturing the forward-scattered light coming from the traps. Variations in the transverse linear momentum can then be related to the changes in the centroid of the intensity distribution and measured by a calibrated position-sensitive detector (PSD) [6, 28, 29].

The force measurement system (Impetux Optics, LUNAM T-40i) must be synchronized with the AWG, considering also the transition time between holograms. In doing so, two clearly different force signals are obtained, one for each group of traps. Since the traps within each group are permanent, the instrument collected light scattered by all the microspheres, and the corresponding force was the sum of all the individual elements [6].

Fig. 3(a) shows the different force signals obtained from a drag force measurement. The stage trajectory was driven by a

triangular voltage signal, which made the piezostage move back and forth at a constant speed, applying two predefined force values of opposite sign to the trapped beads. The two sets of traps were time shared at 15 kHz, so each trap configuration was sampled at 7.5 kHz. Using a pure time-sharing approach would reduce the sampling frequency to 2.5 kHz, resulting in a loss of high-frequency information. Different combinations of micro-beads of two different sizes were analyzed in Fig. 3(b), including cases where one or both trap groups were empty, for which no force was measured. All values fell within ± 7% of the theoretical value, which was calculated from the Stoke's law and the experimental parameters: particle size, the buffer viscosity and the velocity of the piezoelectric stage. Hydrodynamic interaction with the coverslip and neighbor microbeads was neglected.

These results confirm that configurations of permanent traps can be time-shared at very high rates while simultaneous measuring external forces acting on them.

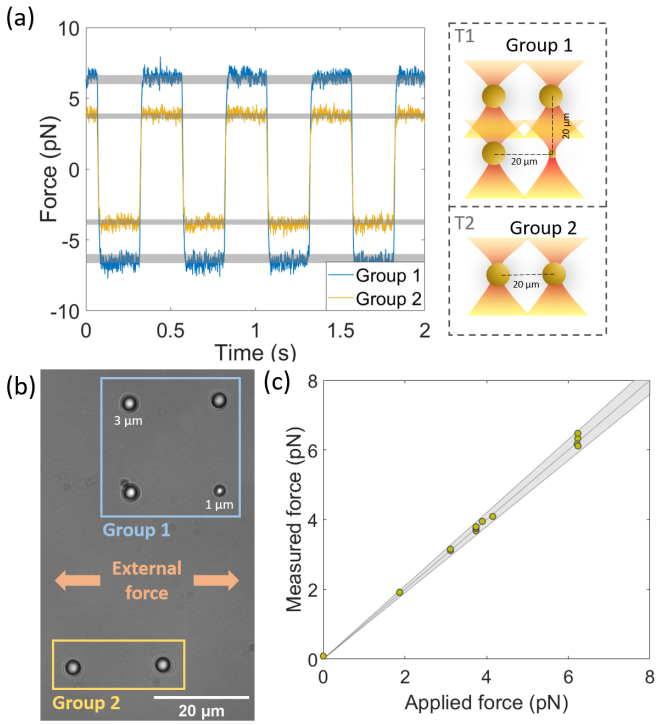

Fig. 3. (a) (Left) Force signals corresponding to each trap group generated with the AODs. Negative values correspond to the stage traveling in the opposite direction. The theoretical force given by Stokes' law is displayed in gray (±7%). (Right) Schematic representation of the trap configurations; the two trap groups were separated 30 µm in order to avoid hydrodynamic interaction between them. (b) Snapshot of the 6 trapped microspheres, indicating the two different trap groups. (c) Comparison of measured and applied force for all drag force measurements. The shaded area corresponds to +/- 5% error.

To conclude, we have demonstrated how a single pair of AODs acting as an SLM can simultaneously exploit both the manipulation capabilities of holographic optical tweezers and the compatibility of time-sharing techniques with laser-based, high-quality position or force measurement methods. Therefore, AHOTs allow us to perform complex experiments in which probing position or force is required at specific sites, even in the presence of other trapped samples or for large/irregular objects that need to be grasped from different points in order to control their position or orientation. AHOTs can be created in a regular setup just by driving the AODs with an AWG, adding this new trap generation capability to the regular time-sharing mode, the user being able to choose the method that best suits the conditions of the experiment.

Funding. *European Union* (Horizon 2020, 777222,); *Generalitat de Catalunya* (2016 LLAV 00022); *University of Barcelona* (F2I-FVal_2018_009, ADR 2015-1016); *Spanish Ministry of Economy and Competitiveness* (BES-2015-074642)

Disclosures. The authors declare no conflicts of interest.

References

1. M. Schingel and M. Bastmeyer, PLOS One **8**, e54850 (2013).
2. M. Polin, D. Grier, and S. Quake, Phys. Rev. Lett. **96**, 088101 (2006).
3. M. Noom, B. V. D. Broek, J. van Mameren, and G. J. L. Wuite, Nat. Methods **4**, 1031–1036 (2007).
4. D. Cojoc et al., PLoS ONE **2**, e1072 (2007).
5. H. Turlier et al., Nat. Phys. **12**, 513 (2016).
6. F. Català, F. Marsà, M. Montes-Usategui, A. Farré, and E. Martín-Badosa, Sci. Rep. **7**, 42960 (2017).
7. J. Liesener, M. Reicherter, T. Haist, and H. J. Tiziani, Opt. Commun. **185**, 77 (2000).
8. J. R. Moffitt, Y. R. Chemla, S. B. Smith, and C. Bustamante, Annu. Rev. Biochem. **77**, 205 (2008).
9. F. Gittes, and C. F. Schmidt, Opt. Lett. **23**, 7 (1998).
10. F. Marsà, A. Farré, E. Martín-Badosa, and M. Montes-Usategui, Opt. Express **21**, 30282 (2013).
11. D. Ott, S. Nader, S. Reihani, and L. B. Oddershede, Opt. Express **22**, 23661 (2014).
12. A. van der Horst, and N. R. Forde, Opt. Express **18**, 7670 (2010).
13. K. Visscher, S. P. Gross, and S. M. Block, IEEE J. Sel. Top. Quantum Electron. **2**, 1066 (1996).
14. D. Ruh, B. Traenkle, and A. Rohrbach, Opt. Express **19**, 21627 (2011).
15. M. Capitanio, R. Cicchi, and F. S. Pavone, Opt. Laser Eng. **45**, 450 (2007).
16. D. L. J. Vossen, A. van der Horst, M. Dogterom, and A. van Blaaderen, Rev. Sci. Instrum. **75**, 2960 (2004).
17. W. H. Guilford, J. A. Tournas, D. Dascalu, and D. S. Watson, Anal. Biochem. **326**, 153 (2004).
18. K. Berg-Sorensen, and H. Flyvbjerg, Rev. Sci. Instrum. **75**, 594 (2004).
19. L. A. Shaw, R. M. Panas, C. M. Spadaccini, and J. B. Hopkins, Opt. Lett. **42**, 2862 (2017).
20. G. M. Akselrod, W. Timp, U. Mirsaidov, Q. Zhao, C. Li, R. Timp, K. Timp, P. Matsudaira, and G. Timp, Biophys. J. **91**, 3465 (2006).
21. T. Čižmár, H. I. C. Dalgarno, P. C. Ashok, F. J. Gunn-More, and K. Dholakia, J. Optics **13**, 044008 (2011).
22. J. W. Goodman, *Introduction to Fourier Optics* (McGraw-Hill, 1996).
23. D. W. Prather, and J. N. Mait, Opt. Lett. **16**, 1720 (1991).
24. E. Tervonen, A. T. Friberg, J. Westerholm, J. Turunen, and M. R. Taghizadeh, Opt. Lett. **16**, 1274 (1991).
25. W. Akemann, J. Léger, C. Ventalon, B. Mathieu, S. Dieudonné, and L. Bourdieu, Opt. Express **23,** 28191 (2015).
26. R. W. Gerchberg, and W. O. Saxton, Optik **35**, 237 (1971).
27. H. Andrews, and C. Patterson, IEEE T. Commun. **24**, 425 (1976).
28. A. Farré, and M. Montes-Usategui, Opt. Express **18**, 11955 (2010).
29. A. Farré, F. Marsà, and M. Montes-Usategui, in *Optical Tweezers: Methods and Protocols* (Springer New York , 2017), p. 41.

Full references

1. M. Schingel, and M. Bastmeyer, "Force Mapping during the Formation and Maturation of Cell Adhesion Sites with Multiple Optical Tweezers," PLOS One **8**, e54850 (2013).
2. M. Polin, D. Grier, and S. Quake, "Anomalous vibrational dispersion in holographically trapped colloidal arrays," Phys. Rev. Lett. **96**, 088101 (2006).
3. M. Noom, B. V. D. Broek, J. van Mameren, and G. J. L. Wuite, "Visualizing single DNA-bound proteins using DNA as a scanning probe," Nat. Methods **4**, 1031–1036 (2007).
4. D. Cojoc, F. Difato, E. Ferrari, R. B. Shahapure, J. Laishram, et al., "Properties of the force exerted by filopodia and lamellipodia and the involvement of cytoskeletal components," PLoS ONE **2**, e1072 (2007).
5. H. Turlier et al., "Equilibrium physics breakdown reveals the active nature of red blood cell flickering," Nat. Phys. **12**, 513–520 (2016).
6. F. Català, F. Marsà, M. Montes-Usategui, A. Farré, and E. Martín-Badosa, "Extending calibration-free force measurements to optically-trapped rod-shaped samples," Sci. Rep. **7**, 42960 (2017).
7. J. Liesener, M. Reicherter, T. Haist, and H. J. Tiziani, "Multi-functional optical tweezers using computer generated holograms," Opt. Commun. **185**, 77–82 (2000).
8. J. R. Moffitt, Y. R. Chemla, S. B. Smith, and C. Bustamante, "Recent advances in optical tweezers," Annu. Rev. Biochem. **77**, 205–228 (2008).
9. F. Gittes, and C. F. Schmidt, "Interference model for back-focal-plane displacement detection in optical tweezers," Opt. Lett. **23**, 7–9 (1998).
10. F. Marsà, A. Farré, E. Martín-Badosa, and M. Montes-Usategui, "Holographic optical tweezers combined with back-focal-plane displacement detection," Opt. Express **21**, 30282-30294 (2013).
11. D. Ott, S. Nader, S. Reihani, and L. B. Oddershede, "Simultaneous three-dimensional tracking of individual signals from multi-trap optical tweezers using fast and accurate photodiode detection," Opt. Express **22**, 23661-23672 (2014).
12. A. van der Horst, and N. R. Forde, "Power spectral analysis for optical trap stiffness calibration from high-speed camera position detection with limited bandwidth," Opt. Express **18**, 7670-7677 (2010).
13. K. Visscher, S. P. Gross, and S. M. Block, "Construction of multiple-beam optical traps with nanometer resolution position sensing," IEEE J. Sel. Top. Quantum Electron. **2**, 1066-1076 (1996).
14. D. Ruh, B. Traenkle, and A. Rohrbach, "Fast parallel interferometric 3D tracking of numerous optically trapped particles and their hydrodynamic interaction," Opt. Express **19**, 21627–21642 (2011).
15. M. Capitanio, R. Cicchi, and F. S. Pavone, "Continuous and time-shared multiple optical tweezers for the study of single motor proteins," Opt. Laser Eng. **45**, 450-457 (2007).
16. D. L. J. Vossen, A. van der Horst, M. Dogterom, and A. van Blaaderen, "Optical tweezers and confocal microscopy for simultaneous three-dimensional manipulation and imaging in concentrated colloidal dispersions," Rev. Sci. Instrum. **75** 2960-2970 (2004).
17. W. H. Guilford, J. A. Tournas, D. Dascalu, and D. S. Watson, "Creating multiple time-shared laser traps with simultaneous displacement detection using digital signal processing hardware," Anal. Biochem. **326**, 153-166 (2004).
18. K. Berg-Sorensen, and H. Flyvbjerg, "Power spectrum analysis for optical tweezers," Rev. Sci. Instrum. **75**, 594–612 (2004).
19. L. A. Shaw, R. M. Panas, C. M. Spadaccini, and J. B. Hopkins, "Scanning holographic optical tweezers," Opt. Lett. **42**, 2862–2865 (2017).
20. G. M. Akselrod, W. Timp, U. Mirsaidov, Q. Zhao, C. Li, R. Timp, K. Timp, P. Matsudaira, and G. Timp, "Laser-Guided Assembly of Heterotypic Three-Dimensional Living Cell Microarrays," Biophys. J. **91**, 3465–3467 (2006).
21. T. Čižmár, H. I. C. Dalgarno, P. C. Ashok, F. J. Gunn-More, and K. Dholakia "Optical aberration compensation in a multiplexed optical trapping system," J. Optics **13**, 044008 (2011).
22. J. W. Goodman, *Introduction to Fourier Optics* (McGraw-Hill, 1996).
23. D. W. Prather and J. N. Mait, "Acousto-optic generation of two-dimensional spot arrays," Opt. Lett. **16**, 1720-1722 (1991).
24. E. Tervonen, A. T. Friberg, J. Westerholm, J. Turunen, and M. R. Taghizadeh, "Programmable optical interconnections by multilevel synthetic acousto-optic holograms," Opt. Lett. **16**, 1274-1276 (1991).
25. W. Akemann, J. Léger, C. Ventalon, B. Mathieu, S. Dieudonné, and L. Bourdieu, "Fast spatial beam shaping by acousto-optic diffraction for 3D non-linear microscopy," Opt. Express **23,** 28191-28205 (2015).
26. R. W. Gerchberg, and W. O. Saxton, "A practical algorithm for the determination of phase from image and diffraction plane pictures," Optik **35**, 237–246 (1971).
27. H. Andrews and C. Patterson, "Singular Value Decomposition (SVD) Image Coding," IEEE T. Commun. **24**, 425-432 (1976).
28. A. Farré, and M. Montes-Usategui, "A force detection technique for single-beam optical traps based on direct measurement of light momentum changes," Opt. Express **18**, 11955-11967 (2010).
29. A. Farré, F. Marsà, and M. Montes-Usategui, "Beyond the Hookean spring model: direct measurement of optical forces through light momentum changes," in *Optical Tweezers: Methods and Protocols*, *Methods in Molecular Biology* **1486**, 41-76, Arne Gennerich (ed.), Springer New York (2017).